XVII European Conference
ECSMGE 2019
Reykjavík
on Soil Mechanics
and Geotechnical Engineering

Buckling of end-bearing retaining walls in clay

Flambement des murs de soutènement en argile

F. Jansson.
ELU Konsult AB, Stockholm, Sweden

N. Nilsson.
BTB AB, Stockholm, Sweden

A.B. Lundberg.
ELU Konsult AB, Stockholm, Sweden

J. Andersson
PEAB Anläggning AB, Solna, Sweden

ABSTRACT: The design of back-anchored retaining walls in Sweden has traditionally not included global elastic instability of the retaining wall as a possible failure mode. Eurocode 3 part 5 (EN 1993-5) requires design of steel structural members for retaining walls to include the risk of buckling, if the normal force exceeds 4 % of the critical buckling load of the retaining wall. Ground anchors drilled into rock and inclined at a 30-50 degree angle to the vertical plane are used to support retaining walls, resulting in a significant normal force in the retaining wall. This article describes the effects on the load bearing capacity for buckling for such a retaining wall. The model simulations show that the soil has a significant influence on the critical load, especially when the retaining wall base is driven to depths greater than 2 meters below excavation depth. The model simulations suggest that higher utilization, with up to 4 times greater critical load, of the steel members is possible for some specific cases.

RÉSUMÉ: En Suède, la conception des murs de soutènement ancrés au dos n'a traditionnellement pas inclus l'instabilité élastique globale du mur de soutènement comme possibilité de défaillance. L'Eurocode 3, partie 5 (EN 1993-5) requiert la conception d'éléments structurels en acier pour les murs de soutènement afin d'évaluer le risque de flambement si la force normale dépasse 4% de la charge critique de flambement du mur de soutènement. Des ancrages au sol forés dans la roche et inclinés à un angle de 30 à 50 degrés par rapport au plan vertical sont utilisés pour soutenir les murs de soutènement, ce qui crée une force normale importante dans le mur de soutènement. Cet article décrit les effets sur la capacité portante de flambement d'un tel mur de soutènement. Les simulations du modèle montrent que le sol a une influence significative sur la charge critique, en particulier lorsque la base du mur de soutènement est entraînée à des profondeurs supérieures à 2 mètres sous la profondeur d'excavation. Les simulations du modèle suggèrent qu'une utilisation plus élevée des éléments en acier, avec une charge critique jusqu'à 4 fois supérieure, est possible dans certains cas spécifiques.

Keywords: Retaining walls; Critical loads; buckling; finite element model; Eurocode 3.

1 INTRODUCTION

The use of Retaining walls is frequently the preferred method to conduct excavations in dense urban environments. Extensive research has been carried out regarding the performance of retaining walls in ultimate limit state and serviceability limit state e.g. (Powrie 1996,

Simpson 1992, Tatsuoka et al 1996). Most inquiries into the behaviour of retaining walls involve purely sedimentary soil, in which the wall element is embedded in the soil mass. There are some notable exceptions to this type of retaining wall, often arising from a different type of geology. The geological conditions in Sweden and Finland are characterized by the intersection of very hard rock and very soft soils: the bedrock consists of the Precambrian Fennoscandian shield, consisting of very hard crystalline granite or gneiss rock with unconfined compressive strength (UCS) frequently in the range of 150-250 MPa. On the other hand, the very soft Holocene clays covering the bedrock typically has an undrained shear strength of around 10-20 kPa, but in some cases as low as 5 kPa, e.g. (Lundberg & Li 2015, Lundberg 2017). A typical soil strata is shown in Figure 1, with a soft Holocene clay layer covering a till layer which was deposited during the Weichselian glaciation, and the Precambrian bedrock. The clay layers in Eastern Sweden are typically limited to 20 m depth, (Bergdahl et al 2003).
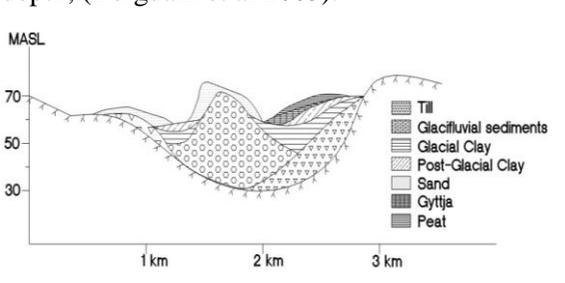

Figure 1. Typical soil strata in Eastern Sweden and Finland.

Piled foundations in these types of soil conditions is normally carried out by driving or drilling piles into the bedrock, and verifying the end-bearing capacity of the pile through dynamic pile load testing, (Andersson et al 2016). Such piles are frequently used as soldier piles in retaining walls; during excavation steel plates are gradually welded to the soldier piles, shown in Figure 2.

Figure 2. Retaining wall consisting of soldier piles and welded steel plates.

Ground anchors for retaining walls are installed through the same method with a tendon drilled and grouted into the bedrock, often with a 45 degree angle, shown in Figure 3. Such anchors can be loaded to the yield strength f_y of the anchor, i.e. the geotechnical capacity of the anchor is not limiting the tensile load. Significant loads are thus transferred to the retaining wall. The vertical component of the anchor load is resisted by the end-bearing piles.
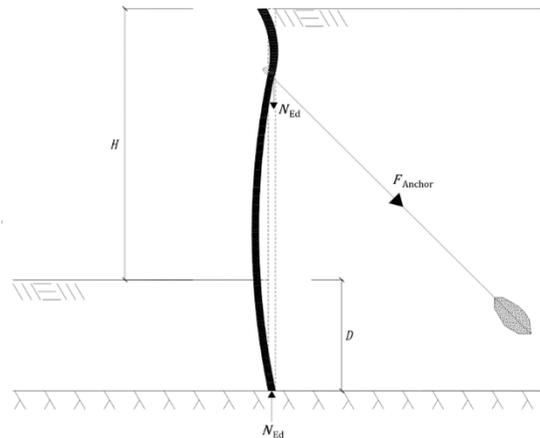

Figure 3. Retaining wall with ground anchor drilled into the Precambrian bedrock.

1.1 Critical load in EN 1993-5

The structural design of the steel components in a retaining wall is governed by Eurocode 3, EN 1993-5, (EC 1993). The normal design load effect N_{Ed} induced into the retaining wall resulting in a possible case of elastic instability with critical load N_{cr} is controlled through the EC-1993 equation 1 and 2.

$$N_{cr} = \frac{\pi^2 EI \beta_D}{l^2} \qquad (1)$$

$$\frac{N_{Ed}}{N_{cr}} \leq 0.04 \qquad (2)$$

In which l is the length between the lower end of the retaining wall and the lowest anchor level, EI is the flexural rigidity of the retaining wall, β_D is a reduction factor for the bending moment resistance of the retaining wall.

If the resulting normal force, N_{Ed}, in the retaining wall is larger than 4% of the critical buckling force, the normal force must be accounted for when calculating the total utilization according to EN 1993-5. The normal force capacity is reduced with regards to the risk of instability using the factor χ which depends on the slenderness of the structure. To accommodate for second order effects the external moment, M_{Ed}, is, in the utilization formula, multiplied by an interaction factor set to 1.15 as can be seen in equation 3.

$$\frac{N_{Ed}}{\chi \cdot N_{Rd}} + 1.15 \cdot \frac{M_{Ed}}{M_{Rd}} \leq 1.0 \qquad (3)$$

When determining the critical buckling load the code specifies two possible models to determine the critical buckling load. Either taking the buckling length as the length from the lowest whale beam to point of sufficient vertical support or 70% of that length if the bottom of the retaining wall is considered as fixed, for instance when drilled into bedrock (EC 1992).

It is stated in EN 1993-5 that a model taking the retaining ability of the surrounding soil into account can be used. A suggested buckling model which takes the soil into account for a retaining wall is however not specified, neither can such a model be found in the literature.

1.2 Critical loads using FEM

Due to a combination of complex geometry and plastic behavior of the soil FEM (finite element method) can be used to determine the buckling behavior of the structure. Several methods exist and the common eigenvalue buckling analysis is a good method to use if one wants a fast determination of the critical load for an ideal elastic structure (Ellobody, Feng, & Young 2014).

Due to the soil reaching its yield deformation quickly and thereafter losing its retaining properties a method taking non-linear effects into account should be used to determine the critical load of a retaining wall. To accommodate these effects a post-buckling analysis, e.g. Riks method, should be performed, where imperfections and plasticity can be included (Novoselac et al. 2012, Crisfield 1981).

The eigenvalue buckling analysis is however also of interest, since the buckled shape from the analysis can be used as an initial imperfection in the post buckling analysis. This can be done using commercial software packages, e.g. ABAQUS, where both a linear eigenvalue buckling analysis and a static Riks analysis can be performed (Dassault Systèmes 2015).

Using a Winkler foundation with non-linear springs both the soils plasticity and the variation of having soil only on one side can be accounted for when determining the crtical load.

2 METHODOLOGY

The analysis of the retaining walls behavior under the influence of a normal load was carried out using non-linear finite element methods, FEM. The model was simplified to one beam representing one of the soldier piles in a retaining wall. Berliner walls with one, two or three anchor

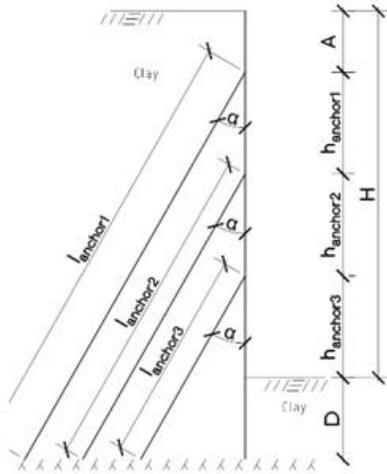levels was used with varying driven depth, D, as described in Figure 4 and Table 1.

Figure 4. Typical cross-section of retaining wall with parameters as presented in Table 1.

For all nine geometrical cases the shear strength of the clay was varied between 7.9 kPa and 78.6 kPa.

The soldier pile was modelled using steel with a yield strength of 460 MPa and a thin walled circular cross-section with a 219.1 mm outer diamter and a thickness of 12.5 mm.

2.1 Modelling

The program ABAQUS 6.14-2 was used for the FEM-modelling and analysis (Dassault Systèmes 2015). Two analysis types were carried out, one linear buckling and one non-linear post-buckling analysis. The linear buckling was used to determine the deformed shape of the structure at the onset of elastic instability. The deformed shape was then used as an initial deformation in the post-buckling analysis.

In both analyses the soil was modelled as Winkler springs with a spring stiffness determined from the subgrade modulus. Linear springs were used in the linear buckling analysis. Figure 5 describes the method used to accomodate for the soil above the excavation bottom on the non-excavated side. A convergence test was used to determine the appropriate distance between the soil springs.

In the post-buckling analysis non-linear springs that only can elongate in one direction were used, either operating in positive or negative direction, depending on the initial buckled shape. Figure 6 describes the layout of the FEM-models both in the linear buckling step and the non-linear post buckling step.

Table 1. specification of the geometrical variations in Figure 3

|	H [m]	D [m]	A [m]	$l_{anchor1}$ [m]	$h_{anchor1}$ [m]	$l_{anchor2}$ [m]	$h_{anchor2}$ [m]	$l_{anchor3}$ [m]	$h_{anchor3}$ [m]	α
	One Anchor Level									
Case 1.1	4	2	1.5	5.2	2.5	-	-	-	-	30°
Case 1.2	4	6	1.5	9.8	2.5	-	-	-	-	30°
Case 1.3	4	10	1.5	14.4	2.5	-	-	-	-	30°
	Two Anchor Levels									
Case 2.1	6.5	2	1.5	8.1	2.5	5.2	2.5	-	-	30°
Case 2.2	6.5	6	1.5	12.7	2.5	9.8	2.5	-	-	30°
Case 2.3	6.5	10	1.5	17.3	2.5	14.4	2.5	-	-	30°
	Three Anchor Levels									
Case 3.1	9	2	1.5	11.0	2.5	8.1	2.5	5.2	2.5	30°
Case 3.2	9	6	1.5	15.6	2.5	12.7	2.5	9.8	2.5	30°
Case 3.3	9	10	1.5	20.2	2.5	17.3	2.5	14.4	2.5	30°
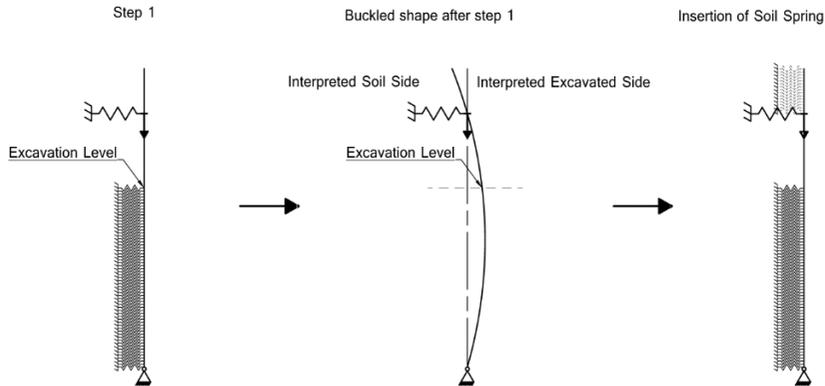
Figure 5. Illustration of method used to decide whether soil-springs would be used above the anchor level.

The inclined anchors were modelled as elastic springs active only in the horisontal direction with a spring stiffness corresponding to its inclination and length for the specific case as presented in Table 1. The effective cross-sectional area of the anchors was set to 1835 mm^2.

2.1.1 Load and boundary conditions

The vertical force was applied as point loads at the anchor levels. In the linear buckling analysis the magnitude of the individual loads was set

proportional to its anchor stiffness so that the total load applied was 1. In the non-linear post buckling analysis the resulting linear buckling load was distributed using the same stiffness proportions.

In the bottom of the soldier pile a pinned support was used to represent the rock support.

2.2 Simulation processing

In the post buckling analysis both elastic and elasto-plastic properties for the steel was used.
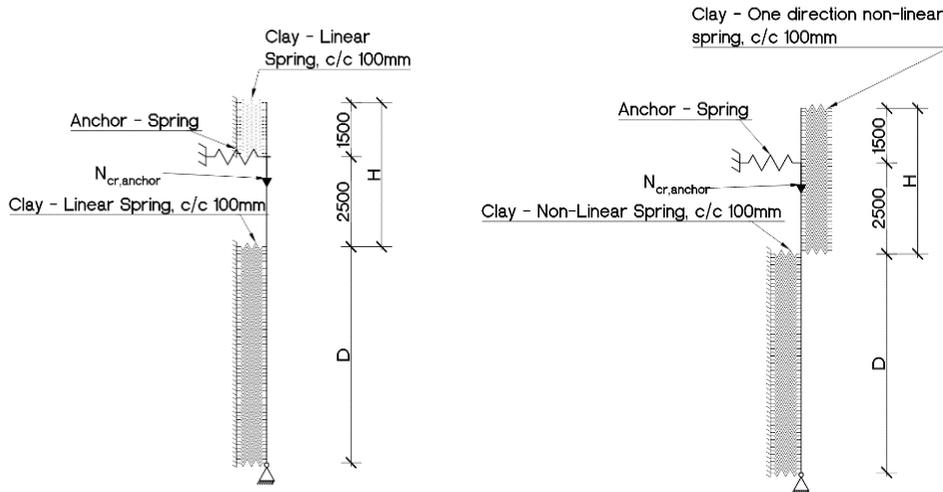

Figure 6. Principle of one anchor level linear buckling (left) and post-buckling (right) model.

The elastic properties were used to attain a full buckling behavioral load-deformation curve.

The elasto-plastic properties were used to determine the normal force capacity of the retaining wall. The normal force capacity attained from the post buckling analysis was compared to normal force capacity attined from the Eurocode calculation for the corresponding case, as presented in equation 4.

$$\frac{N_{pl.Rd.ab}}{\chi \cdot N_{pl.Rd}} \qquad (4)$$

$N_{pl.Rd.ab}$ is the ultimate load reached in the ABAQUS simulation, χ is the reduction factor calcualted according to 6.3.1.2 in EN 1993-1-1, using buckling curve d and $N_{pl.Rd}$ is the yield strength times cross-sectional area.

3   RESULTS

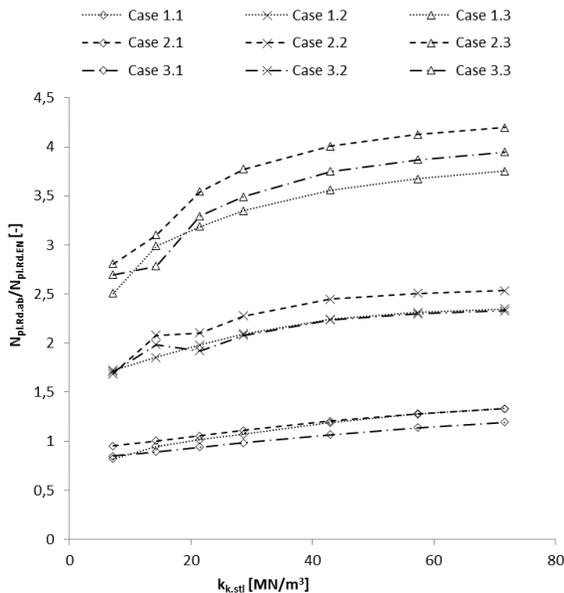In Figure 7 the load proportionality factor, calculated using equation 4, for each case and subgrade modulus is presented.

Figure 7. The ultimate load reached for all cases and corresponding subgrade modulus, k_k, compared to ultimate load according to EN 1993-5.

3.1   Buckling behavior

The general behavior of the soldier pile under the influence of a vertical force is presented as load-deformation curves in Figure 8. Only Case 1.1 is presented with the full shear strength spectrum.
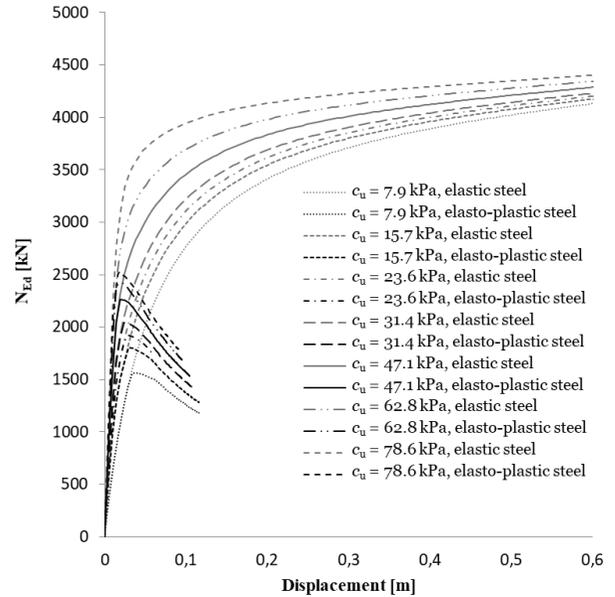
Figure 8. The load-displacement curves from the post buckling models of case 1.1 with various clay shear strength.

4   DISCUSSION

The ultimate loads during buckling presented in Figure 7 show that the configuration of the retaining wall as well as the properties of the surrounding soil has a significant influence on the resistance to global stability of the pile. Since the ultimate loads in Figure 7 are normalized, the calculations results show a large difference between the idealized method without soil support recommended in EN-1993-5 and the beam-spring model outlined in the current paper. There are several parameters which govern the load factor for the parameter study described in Table 1. An initial conclusion is that the normalized load factor agrees well when the driven depth of the pile in the ground is small, but this is to be expected, since the stabilising action

of the soil is then less significant compared to the other cases shown in Table 1. The difference in normalized load factor consequently increases with the driven depth beneath the excavation base as well as the subgrade modulus, shown in Figure 7 and 8.

The main difference between the model recommended in EN 1993-5 and the current beam-spring model is the soil support, and the results are therefore expected. It is therefore of interest to assess how well the current model represent the soil-structure interaction. The representation of the retaining wall pile as a beam element should result in a suitable model according to industry standards, (Simpson 1992). The numerical model is somewhat simplified, and the real 3D soil support is represented by the Winkler springs. However, such idealised elastic springs have been used in practical design in e.g. Powrie (1996) and have been shown to result in a decent representation of reality. The soil-structure interaction is therefore assumed to be reasonably correct and the the main uncertainty lies in the input parameters.

The idealisation of the geological strata presented in Figure 1 shows a layer of till above the bedrock which is often present in Eastern Sweden. This till layer increases the subgrade reaction against the pile, and also increases the rotational resistance at the tip of the pile, further increasing the bearing capacity regarding global instability. A suitable methodology in practical design of retaining walls is to adapt a design soil strata with somewhat conservative soil strength and consider the model refined enough to produce a conservative estimate of the bearing capacity.

5 CONCLUSIONS

The simplified idealised calculation model described in Eurocode EN-1993-5 consist of a buckling model that does not take the support of the surrounding soil against global instability of the pile into accout. In most countries in Europe the soil is sufficiently stiff to resist the global instability failure model and this is not a design issue. However, the very soft Holocene soils and the very hard precambrian rock in Sweden presents conditions in which the global instability is of interest in practical design. The current model shows that simplified model described in EN 1993-5 can be improved, and suggest the available increase in bearing capacity if the surrounding soil is taken into acount in the calculation model.

6 ACKNOWLEDGEMENTS

7 REFERENCES

Andersson, J., Axelsson G., Lundberg, A.B. 2016. Reliability of piles and pile groups based on dynamic load testing. *Proceedings of the 17th Nordic Geotechnical Meeting*, Challenges in Nordic Geotechnic, NGM2016.

Bergdahl, U., Larsson, R., Viberg, L. 2003. Ground investigations and parameter assessment for different geological deposits in Sweden. *In-Situ Characterization of Soils*. KR Saxena and VM Sharma, ed., AA Balkema Publishers, 119-170.

Crisfield, M.A. 1981. A Fast Incremental/ Iterative Solution Procedure That Handles Snap-Through. *Computers & Structures*, **13**, 55-62.

Dassault Systemes. 2015. ABAQUS 6.14 Documentation–Theory Guide. Providence, RI.

Day, R. A., Potts, D. M. 1993. Modelling sheet pile retaining walls. *Computers and Geotechnics*, **15**(3), 125-143.

European Committee for Standardization. 1992. EN-1993. Eurocode 3: Design of steel structures. CEN.

Ellobody, E., Feng, R., Young, B. 2014. Finite Element Analysis and Design of Metal Structures. Waltham: Elsevier.

Lundberg, A. B., Li, Y. 2015. Probabilistic characterization of a soft Scandinavian clay supporting a light quay structure. Geotechnical safety and risk V. IOS Press, Amsterdam, 170-175.

Lundberg, A. B. 2017. Sample Disturbance in Deep Clay Samples. *Landslides in Sensitive Clays*. Springer, Berlin, 133-143.

Novoselac, S., Ergić, T., Baličević, P. 2012. Linear and Nonlinear Buckling and Post Buckling Analysis of a Bar With the Influence of Imperfections. *Tehnički vjesnik*, **19**(3), 695-701.

Potts, D. M., Day, R. A. 1990. Use of sheet pile retaining walls for deep excavations in stiff clay. *Proceedings of the Institution of Civil Engineers*, **88**(6), 899-927.

Powrie, W. 1996. Limit equilibrium analysis of embedded retaining walls. *Géotechnique*, **46**(4), 709-723.

Simpson, B. 1992. Retaining structures: displacement and design. *Géotechnique*, **42**(4), 541-576.

Tatsuoka, F., Tateyama, M., Koseki, J. 1996. Performance of soil retaining walls for railway embankments. *Soils and Foundations*, **36**, 311-324.